JOC Article
pubs.acs.org/joc

Origins of Stereoselectivity in the α-Alkylation of Chiral Hydrazones

Elizabeth H. Krenske,[†,‡] K. N. Houk,*[,†] Daniel Lim,[§] Sarah E. Wengryniuk,[§] and Don M. Coltart*[,§]

[†]*Department of Chemistry and Biochemistry, University of California, Los Angeles, California 90095, United States,* [‡]*School of Chemistry, The University of Melbourne, VIC 3010, Australia, and Australian Research Council Centre of Excellence for Free Radical Chemistry and Biotechnology, and* [§]*Department of Chemistry, Duke University, Durham, North Carolina 27708, United States*

houk@chem.ucla.edu; don.coltart@duke.edu

Received October 7, 2010

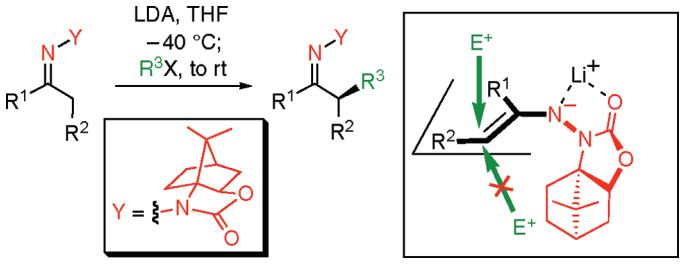

Density functional theory calculations and experiment reveal the origin of stereoselectivity in the deprotonation−alkylation of chiral *N*-amino cyclic carbamate (ACC) hydrazones. When the ACC is a rigid, camphor-derived carbamate, the two conformations of the azaenolate intermediate differ in energy due to conformational effects within the oxazolidinone ring and steric interactions between the ACC and the azaenolate. An electrophile adds selectively to the less-hindered π-face of the azaenolate. Although it was earlier reported that use of ACC auxiliaries led to α-alkylated ketones with er values of 82:18 to 98:2, B3LYP calculations predict higher stereoselectivity. Direct measurement of the dr of an alkylated hydrazone prior to removal of the auxiliary confirms this prediction; the removal of the auxiliary under the reported conditions can compromise the overall stereoselectivity of the process.

Introduction

The α-alkylation of ketones is a useful synthetic operation, most often achieved via electrophilic addition to a derived azaenolate. Compared with enolates, azaenolates provide improved reactivities, yields, and regioselectivities and can incorporate nitrogen-based chiral auxiliaries.[1] Enders' SAMP/RAMP auxiliaries, the proline-based (*S*)- and (*R*)-1-amino-2-methoxymethylpyrrolidines (Scheme 1), are widely used.[1f,g] An attractive feature of the SAMP/RAMP methodology is the well-defined stereochemical predictability; the appropriate enantiomer of the auxiliary can be chosen in advance. There have been many studies, both experimental and theoretical, of the mechanisms and stereoselectivities of alkylations of azaenolates derived from dialkylhydrazones, imines, and oximes.[2]

We recently discovered that chiral *N*-amino cyclic carbamate (ACC) auxiliaries are convenient alternatives for ketone α-alkylations (Scheme 2).[3] ACCs react easily with ketones to

(1) (a) Meyers, A. I.; Williams, D. R.; Druelinger, M. *J. Am. Chem. Soc.* **1976**, *98*, 3032–3033. (b) Meyers, A. I.; Williams, D. R. *J. Org. Chem.* **1978**, *43*, 3245–3247. (c) Meyers, A. I.; Williams, D. R.; Erickson, G. W.; White, S.; Druelinger, M. *J. Am. Chem. Soc.* **1981**, *103*, 3081–3087. (d) Hashimoto, S.; Koga, K. *Tetrahedron Lett.* **1978**, *19*, 573–576. (e) Hashimoto, S.; Koga, K. *Chem. Pharm. Bull.* **1979**, *27*, 2760–2766. (f) Enders, D. In *Asymmetric Synthesis*; Morrison, J. D., Ed.; Academic Press: Orlando, 1984; Vol. 3, Part B, pp 275−339. (g) Job, A.; Janeck, C. F.; Bettray, W.; Peters, R.; Enders, D. *Tetrahedron* **2002**, *58*, 2253–2329.

(2) (a) Dialkylhydrazones: Boche, G. *Angew. Chem., Int. Ed. Engl.* **1989**, *28*, 277–297. Collum, D. B.; Kahne, D.; Gut, S. A.; DePue, R. T.; Mohamadi, F.; Wanat, R. A.; Clardy, J.; Van Duyne, G. *J. Am. Chem. Soc.* **1984**, *106*, 4865–4869. Enders, D.; Eichenauer, H.; Baus, U.; Schubert, H.; Kremer, K. A. M. *Tetrahedron* **1984**, *40*, 1345–1359. Ludwig, J. W.; Newcomb, M.; Bergbreiter, D. E. *J. Org. Chem.* **1980**, *45*, 4666–4669. Lazny, R.; Nodzewska, A. *Chem. Rev.* **2010**, *110*, 1386–1434. (b) Imines: Fraser, R. R.; Banville, J.; Dhawan, K. L. *J. Am. Chem. Soc.* **1978**, *100*, 7999–8001. Hosomi, A.; Araki, Y.; Sakurai, H. *J. Am. Chem. Soc.* **1982**, *104*, 2081–2083. Smith, J. K.; Bergbreiter, D. E.; Newcomb, M. *J. Am. Chem. Soc.* **1983**, *105*, 4396–4400. Houk, K. N.; Strozier, R. W.; Rondan, N. G.; Fraser, R. R.; Chuaqui-Offermanns, N. *J. Am. Chem. Soc.* **1980**, *102*, 1426–1429. (c) Oximes: Kofron, W. G.; Yeh, M.-K. *J. Org. Chem.* **1976**, *41*, 439–442. Glaser, R.; Streitwieser, A. *J. Am. Chem. Soc.* **1987**, *109*, 1258–1260. Kallman, N.; Collum, D. B. *J. Am. Chem. Soc.* **1987**, *109*, 7466–7472. Glaser, R.; Streitwieser, A., Jr. *J. Am. Chem. Soc.* **1989**, *111*, 7340–7348.

(3) Lim, D.; Coltart, D. M. *Angew. Chem., Int. Ed.* **2008**, *47*, 5207–5210.

Published on Web 11/11/2010 DOI: 10.1021/jo1019877

SCHEME 1. Stereoselective α-Alkylation of a RAMP Hydrazone[1g]

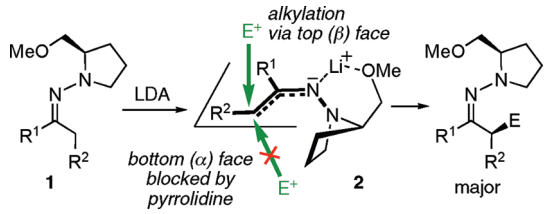

SCHEME 2. Asymmetric α-Alkylation of Ketones Mediated by ACC 4

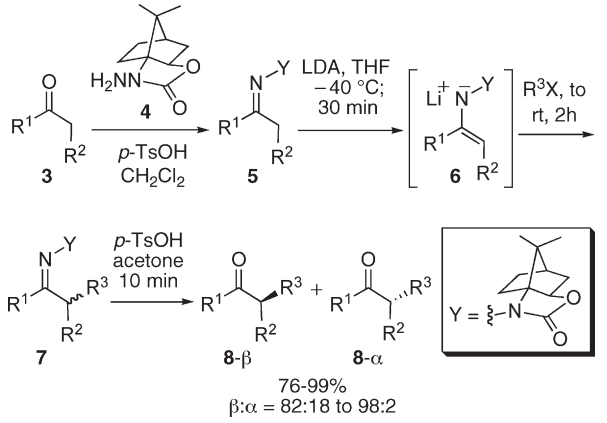

SCHEME 3. Model Proposed To Explain Stereoselectivity in the Alkylation of ACC Hydrazones[3]

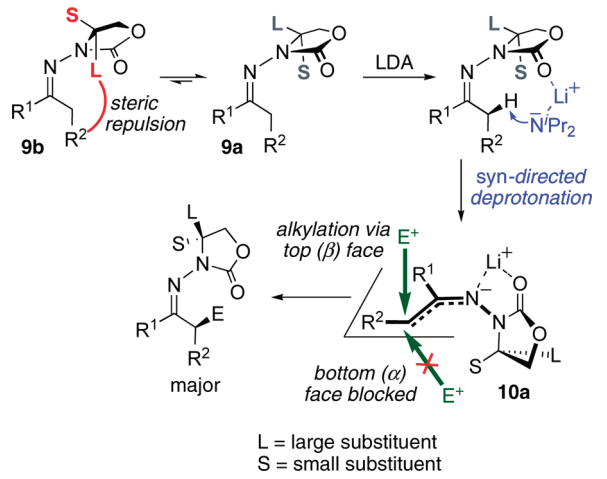

afford hydrazones and can be recovered quantitatively from the products after alkylation. Deprotonation of an ACC hydrazone is rapid; the stereoselectivity of alkylation is high even without the use of extreme low temperature, and yields are excellent. Among the ACCs that we have investigated to date, camphor-based auxiliary **4** (Scheme 2) has proven to give the best yields and enantioselectivities.

A mechanism for the stereoselective alkylation of a SAMP/RAMP hydrazone was proposed by Enders on the basis of crystallographic, spectroscopic, and computational evidence[1g,4,5] and is depicted in Scheme 1. Kinetic deprotonation of hydrazone **1** gives rise to lithium azaenolate **2** which, following equilibration, has the *E*-configuration at the CC bond and the *Z*-configuration at the CN bond.[6] The bottom face of **2** is blocked by the pyrrolidine ring, and reaction with an electrophile takes place selectively at the top (*β*) face.[7]

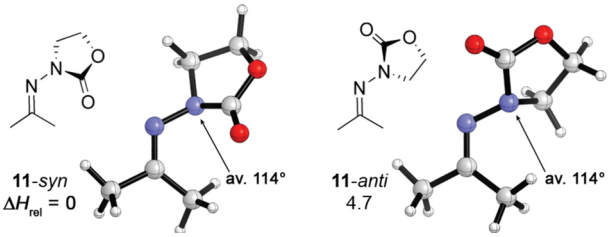

FIGURE 1. Conformers of the ACC hydrazone **11** (Δ*H* in kcal mol^{-1} at 0 K).

We proposed[3] that a similar mechanism is followed in the alkylation of an ACC azaenolate but that the formation of the azaenolate from the hydrazone is controlled by the orientation of the carbonyl group. As shown in Scheme 3, the generalized ACC hydrazone **9** would prefer to exist in the conformation depicted as **9a**, where steric interactions between R^2 and the larger substituent (L) on the auxiliary are minimized. Coordination of LDA to the carbonyl group would then lead to a "*syn*-directed" deprotonation,[8] giving the E_{CC}/Z_{CN}-azaenolate **10a** as a five-membered chelate. The bottom face of **10a** is sterically blocked, and alkylation should take place selectively at the top (*β*) face.

We present here a computational study of the deprotonation of ACC hydrazones and the alkylation of the lithium azaenolates. Density functional theory calculations provide information about the transition states that lead to the selectivities shown in Scheme 2. However, computations predict even higher stereoselectivities than were originally reported.[3] This discovery prompted us to measure directly the dr of an alkylated hydrazone, prior to its conversion to the ketone. Consistent with theoretical predictions, the dr of the hydrazone was higher than the er of the final ketone, revealing that the removal of the auxiliary indeed compromised the overall stereoselectivity of the process.

Results and Discussion

To explore the structural properties of ACC hydrazones, we first examined the parent ACC hydrazone **11** (Figure 1). At the B3LYP/6-31G(d) level, two isomers of **11** were located, which differ in the conformation about the N−N bond. The more stable isomer, **11**-*syn*, has a synclinal arrangement of the N−$C_{C=O}$ bond and the N=C bond ($CNNC_{C=O}$ dihedral angle 71°). The other isomer (**11**-*anti*) has an *anti* arrangement of these bonds (dihedral angle 150°) and is 4.7 kcal mol^{-1} less stable (ΔH_{0K}). Its lower stability is

(4) (a) Enders, D.; Eichenauer, H. *Angew. Chem., Int. Ed. Engl.* **1976**, *15*, 549–551. (b) Enders, D.; Eichenauer, H. *Tetrahedron Lett.* **1977**, *18*, 191–194.
(5) Enders, D. *Chem. Scripta* **1985**, *25*, 139–147.
(6) Davenport, K. G.; Eichenauer, H.; Enders, D.; Newcomb, M.; Bergbreiter, D. E. *J. Am. Chem. Soc.* **1979**, *101*, 5654–5659.
(7) For an X-ray crystal structure of the lithium azaenolate derived from treatment of 2-acetylnaphthalene-SAMP hydrazone with LDA, see: Enders, D.; Bachstädter, G.; Kremer, K. A. M.; Marsch, M.; Harms, K.; Boche, G. *Angew. Chem., Int. Ed. Engl.* **1988**, *27*, 1522–1524.
(8) For a review of metal-mediated complex-induced proximity effects in deprotonation, see: Whisler, M. C.; MacNeil, S.; Snieckus, V.; Beak, P. *Angew. Chem., Int. Ed.* **2004**, *43*, 2206–2225.

SCHEME 4. Average Bond Angles at Nitrogen in Model Species

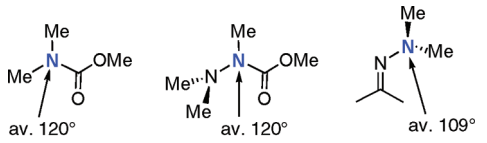

due to repulsive interactions between the C=N and C=O lone pairs. In both isomers of the hydrazone, the ring nitrogen is pyramidal with an average bond angle of 114°. In this respect, the ACC hydrazone differs from simple carbamates (cf. species **12** and **13**, Scheme 4) and instead resembles an *N*,*N*-dialkylhydrazone (**14**). The NR_2 lone pair in **11** and **14** lies roughly in the same plane as the C=N bond, as a result of steric effects.[9]

To study the directed deprotonation of **11**, Li(NMe_2)(THF) was used as a model for LDA in THF solution. Both **11**-*syn* and **11**-*anti* can undergo an intramolecular deprotonation reaction, following coordination of Li(NMe_2)(THF) to the carbonyl oxygen. The transition states, **TS-11**-*syn* and **TS-11**-*anti*, are shown in Figure 2. The reaction involving **11**-*syn* represents the "*syn*-directed" deprotonation described above (Scheme 3), whereas the reaction of **11**-*anti* leads to the opposite result, formation of a carbanion *trans* to the ACC group. The "*syn*-directed" deprotonation pathway is favored: **TS-11**-*syn* lies 1.4 kcal mol^{-1} lower than **TS-11**-*anti*. The absolute barriers, relative to the reactant complexes, are very low or negative in the gas phase ($\Delta H^{\ddagger}$ = 0.3 and −0.6 kcal mol^{-1}, respectively). Because the lowest-energy TS (**TS-11**-*syn*) appears to have a vacant coordination site on the lithium, we reoptimized its geometry with a second THF coordinated. The second THF was found to bind in a slightly endergonic fashion (ΔG +2.4 kcal mol^{-1} relative to **TS-11**-*syn* + THF). For the *anti* geometry, the lithium is already 4-coordinate in **TS-11**-*anti*, and a stable structure containing a second THF could not be located.

For the chiral hydrazone **15**, derived from the ACC **4**, there are four classes of conformational isomers. These are shown in Figure 3a. Unlike the achiral hydrazone **11**, **15** can only adopt a *syn* conformation. Steric crowding between the rigid bicycloalkane unit and the hydrazone α-methyl group is too severe for *anti* conformers to be energy minima. The two *syn* conformers, **15**-*syn*-front and **15**-*syn*-back, correspond to the proposed structures **9a** and **9b** of Scheme 3, respectively (the terms "front" and "back" refer to the orientation of the carbonyl group). Consistent with the earlier model,[3] **15**-*syn*-front is 3.5 kcal mol^{-1} more stable than **15**-*syn*-back. The destabilization of **15**-*syn*-back can be traced to the conformation about the N−C_4 bond in the oxazolidinone ring. Although the two conformers of **15**-*syn* are formally related by rotation about the N−N bond, their interconversion also induces a change in configuration at the ring nitrogen. This is depicted in Figure 3b, which shows Newman projections along the N−C_4 bond after the N=CMe_2 group has been replaced by a hydrogen atom (green). The N−C_4 bond in **15**-*syn*-back shows substantial eclipsing, with CNCC and NNCC dihedral angles of 12° and

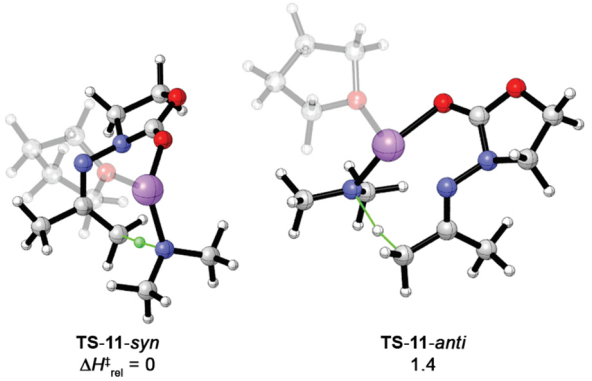

FIGURE 2. Transition states for deprotonation of **11** by Li(NMe_2)(THF). THF ligands are fogged out for clarity. The "*syn*-directed" deprotonation, leading to the Z_{CN} azaenolate, is favored ($\Delta H^{\ddagger}_{rel}$ in kcal mol^{-1} at 0 K).

22°, respectively. By contrast, the smallest dihedral angles about N−C_4 in **15**-*syn*-front are 29° and 56°. The energy difference between the two structures in Figure 3b is 2.2 kcal mol^{-1} (ΔE).

Transition states for the deprotonation of **15** by coordinated Li(NMe_2)(THF) are shown in Figure 4. The relative energies of the transition states are the same as those of the hydrazones themselves; **TS-15**-*syn*-front is 3.5 kcal mol^{-1} lower in energy than **TS-15**-*syn*-back. The barriers relative to reactants (0.5 and 1.1 kcal mol^{-1}, respectively) are similar to those for the achiral **TS-11**-***syn*** and **TS-11**-***anti***. The eclipsing interactions about N−C_4 that were present in **15**-*syn*-back are also present in **TS-15**-*syn*-back. There is also a destabilizing steric interaction (shown by the red line) between the hydrazone α-methyl group and the nearby methyl group on the auxiliary. The chiral ACC effectively blocks *anti* deprotonation and makes the front (β) deprotonation considerably easier than the back (α). The front/back selectivity is calculated to be only marginally affected by solvation. When the transition structures were optimized in THF using the conductorlike polarizable continuum model (CPCM),[10,11] the preference for **TS-15**-*syn*-front was $\Delta\Delta H^{\ddagger}$ = 3.3 kcal mol^{-1} ($\Delta\Delta G^{\ddagger}$ = 4.2 kcal mol^{-1} at 298.15 K). A transition state related to **TS-15**-*syn*-front but containing a second THF in the coordination sphere of Li^+ was found to be 1.9 kcal mol^{-1} less stable (ΔG) in the gas phase.

The overall stereoselectivity of the deprotonation−alkylation sequence is determined by the addition of the azaenolate to the electrophile. The geometry of lithium azaenolate **16** and transition states for its reaction with MeCl are shown in Figure 5. Two THF ligands were included in the coordination sphere of Li^+. During the alkylation, the ACC can be oriented with its carbonyl group lying in front of or behind the plane of the azaenolate. MeCl can add to either conformer and can approach from either the front or back. Figure 5 shows four transition states, which correspond to these four possible arrangements of the ACC and MeCl with respect to the plane of the azaenolate. The relative enthalpies and free energies are given below each transition state, both for the gas phase and with a THF solvent model in addition to the two explicit THFs.

(9) (a) Karabatsos, G. J.; Taller, R. A.; Vane, F. M. *Tetrahedron Lett.* **1964**, *5*, 1081–1085. (b) Karabatsos, G. J.; Taller, R. A. *Tetrahedron* **1968**, *24*, 3923–3937.

(10) Barone, V.; Cossi, M. *J. Phys. Chem. A* **1998**, *102*, 1995–2001.

(11) Barone, V.; Cossi, M.; Tomasi, J. *J. Comput. Chem.* **1998**, *19*, 404–417.

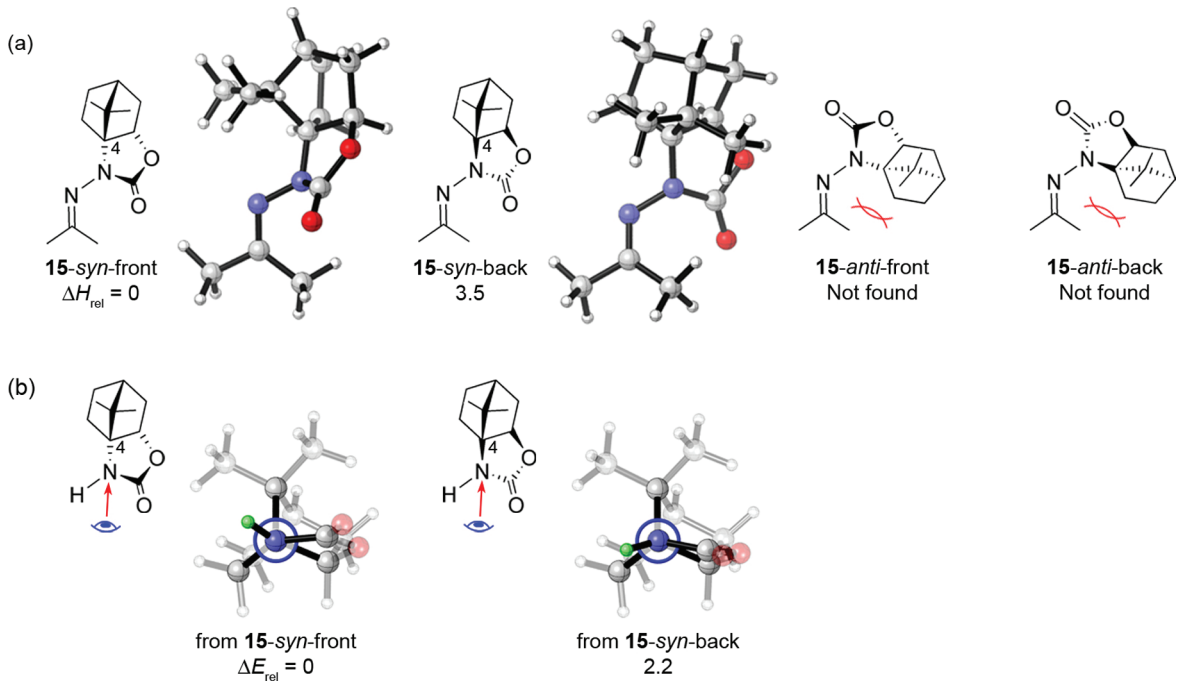

FIGURE 3. (a) Conformers of the hydrazone **15** and (b) Newman projections showing the conformation about the N−C_4 bond in the oxazolidinone ring [N=CMe_2 unit has been removed and replaced by H (green) at a distance of 1 Å, while the remaining atoms were held fixed]. Only the *syn* conformation is available to **15**, because the *anti* conformers would be subject to severe steric interactions between the auxiliary and the nearby alkyl group on the hydrazone. The rigid bicycloalkane moiety enforces destabilizing eclipsing interactions about the N−C_4 bond in **15**-*syn*-back.

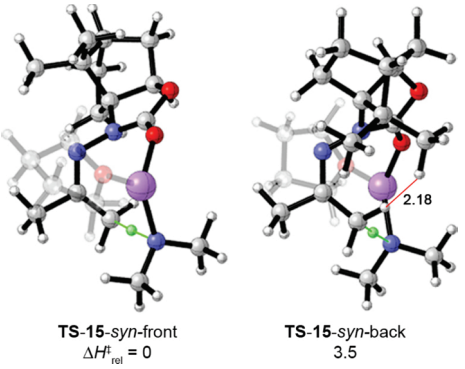

FIGURE 4. Transition states for deprotonation of **15** by Li(NMe_2)(THF). Deprotonation from the front (β) face is favored. The transition state for deprotonation from the back is destabilized both by eclipsing interactions about N−C_4 and by steric interactions between the hydrazone and the auxiliary (red line) (interatomic distances in Å).

The lithium azaenolate **16** is subject to the same conformational effects described above for the corresponding hydrazone **15**. The ring nitrogen is less pyramidal than in the corresponding hydrazone, with an average bond angle of 117° in **16**-front and 118° in **16**-back. Pyramidalization (109°) at the ring nitrogen has previously been observed in the crystal structure of the SAMP hydrazone **17**.[7] The lithium azaenolate **16**-back, like its hydrazone precursor, is destabilized by eclipsing interactions about the N−C_4 bond. **16**-back is also destabilized by steric interactions between the azaenolate and one of the methyl groups on the auxiliary (red line in Figure 5a), similar to those present in the TS for its formation (**TS-15**-*syn*-back, Figure 4). These two effects destabilize **16**-back by 5 kcal mol^{-1} relative to **16**-front. The front-back difference increases to 7 kcal mol^{-1} in their TSs for reaction with MeCl. Additionally, regardless of the conformation of **16**, there is also a 7 kcal mol^{-1} preference for MeCl to add to the π-face where the carbonyl group (coordinated to Li^+) is located (**TS-16-A**, **TS-16-D**). Addition to the opposite face (**TS-16-B**, **TS-16-C**) is disfavored because of steric repulsion between MeCl and the bicycloalkane group, as indicated by the red lines in Figure 5b. Thus, the alkylation of **16** takes place exclusively through the lower-energy conformer **16**-front, and MeCl adds selectively to the front side (**TS-16-A**). The large stereochemical preference is the result of both steric effects and $Li^+\cdots Cl^-$ attraction in **TS-16-A**.

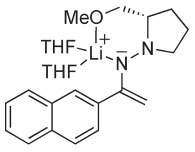

17

Having established the facial selectivity of alkylation at an unsubstituted azaenolate terminus, we then investigated the alkylation of a substituted azaenolate. Deprotonation at a secondary carbon introduces the additional consideration of E_{CC}/Z_{CC} selectivity. We suggested earlier[3] that E_{CC} azaenolates are formed preferentially, on the basis that the allylation of a 3-pentanone-derived hydrazone and a cyclohexanone-derived hydrazone both led to ketones that had the same configuration at the newly formed stereocenter. Transition states for the deprotonation of an unsymmetrical hydrazone (**18**) by Li(NMe_2)(THF) are shown in Figure 6. The calculated

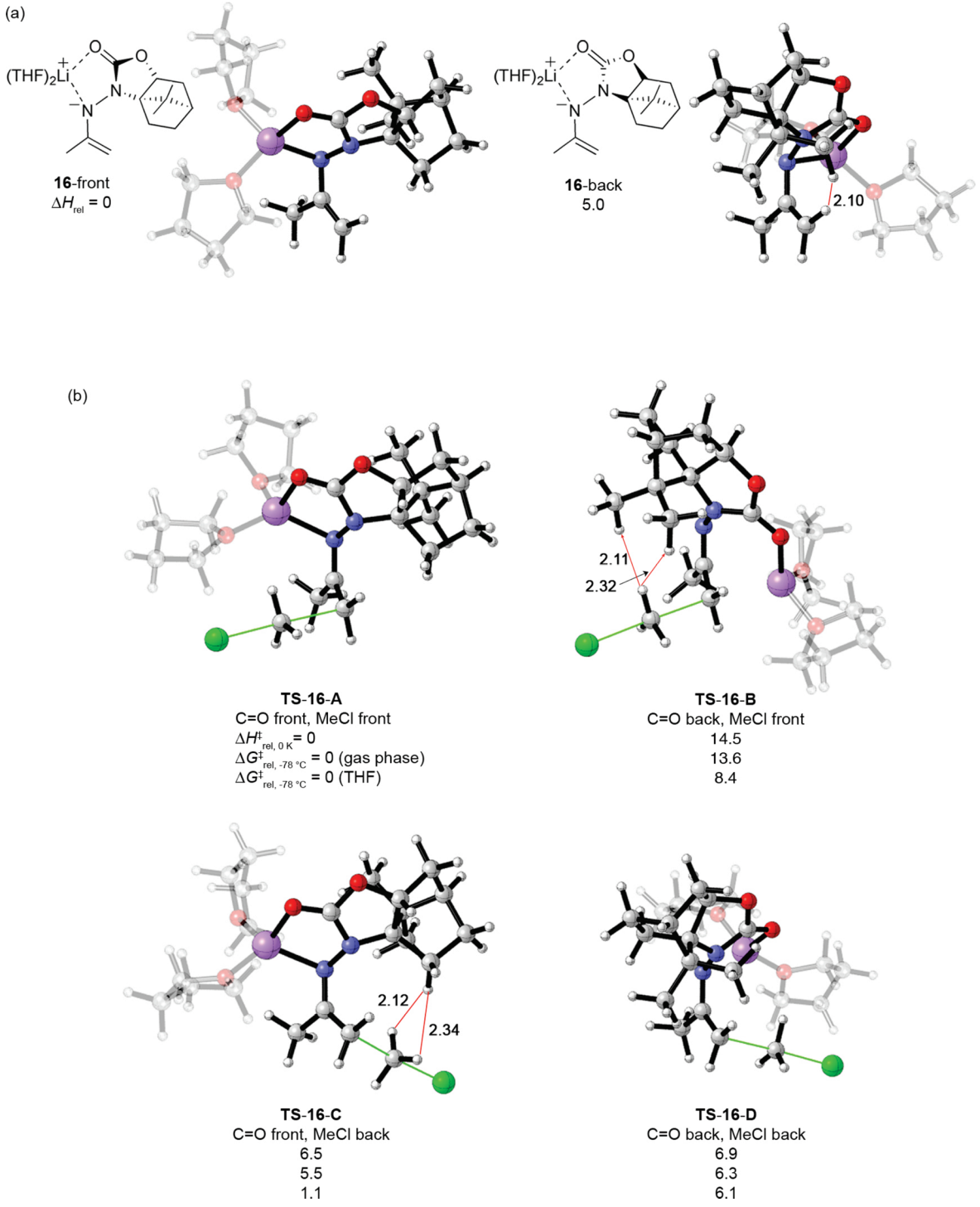

FIGURE 5. (a) Conformers of the lithium azaenolate **16** and (b) transition states for alkylation of **16** by MeCl. Both the azaenolate and the TSs for alkylation prefer the carbonyl-front conformation. Addition of MeCl to the β face of the azaenolate (**TS-16-A**) is preferred by 6.5 kcal mol^{-1} over addition to the α face (**TS-16-C**) in the gas phase. A similar but smaller preference is retained in solution.

barriers confirm the E_{CC} selectivity. The TS leading to azaenolate **19**-E_{CC} is favored by 2.9 kcal mol^{-1} over the TS leading to **19**-Z_{CC}. Similar selectivity for formation of E_{CC} azaenolates has previously been established for SAMP/RAMP-hydrazones.[6]

Once formed, the azaenolate **19**-E_{CC} is unlikely to undergo conversion to the Z_{CC} isomer. We calculate a C=C rotational barrier of 43 kcal mol^{-1} for the azaenolate derived from **11**, and the barrier for the more-hindered azaenolate **19**-E_{CC} is likely quite higher. The reaction of **19**-E_{CC} with MeCl is calculated to have a stereoselectivity similar to that of **16**; front-side addition of MeCl to **19**-E_{CC} is favored by 6.9 kcal mol^{-1} ($\Delta\Delta H^{\ddagger}_{0K}$) over back-side addition (Supporting Information).

Although the B3LYP gas-phase calculations for alkylations of **16** and **19**-E_{CC} predict the correct major products,[3] they also predict higher stereoselectivity compared with that

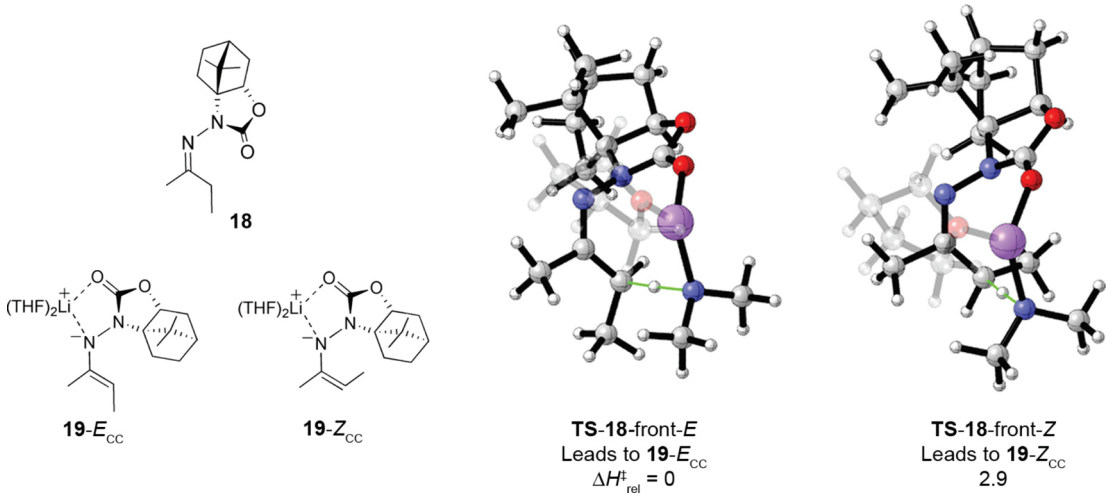

FIGURE 6. Transition states for deprotonation of the substituted hydrazone **18** by Li(NMe$_2$)(THF). The TS leading to the E_{CC} isomer of the azaenolate is 2.9 kcal mol^{-1} lower in energy than the TS leading to the Z_{CC} azaenolate.

reported previously. For example, the allylation of hydrazone **20** with allyl bromide (Scheme 5) was reported to give ketone **22** with an er of 96:4, but the gas-phase activation energies for the reactions of the azaenolates **16** or **19**-E_{CC} with MeCl predict the product **22**-β would be formed exclusively. This high selectivity decreases only slightly with a bulkier electrophile; for example, the alkylation of **16** by EtCl is calculated to have a stereoselectivity of 5.7 kcal mol^{-1} (cf. 6.5 kcal mol^{-1} for MeCl).

The very high predicted gas-phase selectivities prompted us to reappraise the experimental selectivities. In our initial study,[3] er values were determined for the ketone products, following hydrolytic cleavage of the auxiliary. We repeated the allylation of **20** (Scheme 5), and this time measured the *diastereomer ratio* of **21**-β to **21**-α. HPLC analysis revealed that **21**-β and **21**-α were formed in a ratio of >99:1.[12] Subsequent hydrolysis of the auxiliary led to **22**-β and **22**-α in a ratio of 96:4. Thus, despite the reasonably mild conditions and short reaction time, erosion of stereochemical integrity occurs during the hydrolysis. We are now seeking improved conditions for auxiliary cleavage.

The predicted stereoselectivity in solution, however, is nevertheless not as high as in the gas phase. For example, in the reaction of the azaenolate **16** with MeCl, the TS leading to the minor product (**TS-16-C**) has a larger degree of charge transfer to MeCl (0.35 e) than the lowest-energy TS (**TS-16-A**, 0.29 e).[13] This would be expected to lead to enhanced stabilization of the minor TS in solution. We calculated CPCM free energies of solvation for the gas-phase structures in THF. The calculated value of $\Delta\Delta G^{\ddagger}$ in THF at −78 °C is only 1.1 kcal mol^{-1}, corresponding to a dr of 95:5. The same value of $\Delta\Delta G^{\ddagger}$ is obtained if the transition structures are fully optimized in the solvent model. Although this value is not expected to be quantitatively accurate (an accurate treatment of solvent effects would require more sophisticated modeling, including treatment of different coordination states for Li^+) and indeed underestimates the experimental dr, it does indicate that the predicted stereoselectivity is sensitive to solvation.

SCHEME 5. Asymmetric α-Allylation of 20

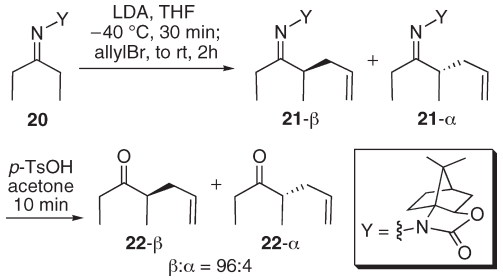

Conclusion

B3LYP calculations support the model for the stereoselectivity of ketone α-alkylation shown in Scheme 3. The crucial features are that (i) the conformation of the intermediate azaenolate is controlled by conformational effects in the oxazolidinone ring and by steric repulsion between the chiral auxiliary and the deprotonated group, and (ii) an electrophile reacts preferentially with the lower-energy azaenolate, from the side opposite the bulky bicycloalkane group. These features resemble the mechanism of stereoinduction in the alkylation of SAMP/RAMP hydrazones.[4,5] ACC hydrazones represent a convenient new complement to the SAMP/RAMP methodology.

Theoretical Calculations

B3LYP calculations[14−16] were performed with Gaussian 03[17] and Gaussian 09.[18] The nature of each optimized point was checked by calculation of the vibrational frequencies, and

(12) No regioisomeric products corresponding to allylation at the α′-position were formed.
(13) Mulliken charges at the B3LYP/6-31G(d) level.

(14) Becke, A. D. *J. Chem. Phys.* **1993**, *98*, 5648–5652.
(15) Stephens, P. J.; Devlin, F. J.; Chabalowski, C. F.; Frisch, M. J. *J. Phys. Chem.* **1994**, *98*, 11623–11627.
(16) Lee, C.; Yang, W.; Parr, R. G. *Phys. Rev. B* **1988**, *37*, 785–789.
(17) Frisch, M. J., et al. *Gaussian 03*, Revision C.02; Gaussian, Inc.: Wallingford, CT, 2004.
(18) Frisch, M. J., et al. *Gaussian 09*, Revision A.02; Gaussian, Inc.: Wallingford, CT, 2009.

transition states were further verified by IRC calculations.[19,20] Zero-point energy and thermal corrections were derived from the B3LYP/6-31G(d) frequencies, scaled by Radom's factors.[21] The effects of basis set size were investigated through calculations of the transition states **TS-11**-*syn* and **TS-11**-*anti* with the 6-311+G(2d,p) basis (leaving frequencies unscaled); this raised the selectivity in favor of **TS-11**-*syn* from 1.4 to 2.9 kcal mol^{-1}, while the bond lengths involving the transferring proton changed by only 0.01−0.02 Å. The effects of solvation were simulated by means of CPCM calculations[10,11] using UAKS radii. Free energies of solvation were calculated for the gas-phase-optimized geometries and were added to the gas-phase free energies to obtain the solution-phase free energies. We also performed geometry optimizations for selected species in THF (Gaussian 09). Solution-phase free energies are quoted at 1 mol L^{-1}. Molecular graphics were produced with the CYLview program.[22] For simplicity, we have only considered monomeric species where the Li^+ is coordinated by one NMe_2^- and one or two THF ligands (for the deprotonation step), or by two THF ligands (for the alkylation step). A fuller treatment would involve adducts having alternative coordination numbers and aggregation states, as well as multiple conformational isomers. Collum[23] has shown, for example, that at high THF concentrations, the lithium azaenolate derived from cyclohexanone phenylimine exists predominantly as a monomeric species with three THF ligands coordinated to Li^+. The structures, aggregation states, and reactivities of lithium enolates and related species have been studied computationally by Pratt.[24] In our simple model complexes, sampling of different THF conformations showed energetic variations amounting to a few tenths of a kcal mol^{-1}.

Experimental Methods

Allylation of 20. *n*-BuLi (2.5 M in hexanes, 100 μL, 0.250 mmol) was added dropwise over ca. 2 min to a stirred and cooled (−78 °C) solution of diisopropylamine (38.2 μL, 0.272 mmol) in THF (1.0 mL) (Ar atmosphere). The mixture was cooled for 30 min with an ice−H_2O bath and then cooled to −40 °C. A solution of **20** (60.0 mg, 0.227 mmol) in THF (1.0 mL) was added by cannula, with additional THF (2 × 0.3 mL) as a rinse, and the mixture was stirred for 45 min. Allyl bromide (23.7 μL, 0.272 mmol) was then added, and stirring was continued for 5 min. The cold bath was removed, and the mixture was stirred for an additional 40 min and then partitioned between Et_2O and H_2O. The aqueous phase was extracted with Et_2O (twice), and the combined organic extracts were washed with brine, dried ($MgSO_4$), filtered, and evaporated under reduced pressure to give crude **21**. ^{1}H NMR ($CDCl_3$, 400 MHz): δ 5.90−5.70 (m, 1H), 5.18−4.94 (m, 2H), 4.25 (dd, J = 8.1, 4.1 Hz, 1H), 3.18−3.04 (m, 1H), 2.50−2.24 (m, 4H), 2.14−1.80 (m, 4H), 1.76 (t, J = 4.4 Hz, 1H), 1.26−1.32 (m, 2H), 1.23 (s, 3H), 1.16 (s, 3H), 1.13 (t, J = 7.2 Hz, 3H), 0.94 (d, J = 7.0 Hz, 3H). HPLC analysis of this material showed a 99.3:0.7 mixture of **21**-β/**21**-α.[25]

The crude material was purified via flash chromatography over silica gel using 10:90 EtOAc/hexanes to give **21** as a pure, light-yellow oil (66 mg, 96%). ^{1}H NMR ($CDCl_3$, 400 MHz): δ 5.90−5.70 (m, 1H), 5.18−4.94 (m, 2H), 4.25 (dd, J = 8.1, 4.1 Hz, 1H), 3.18−3.04 (m, 1H), 2.50−2.24 (m, 4H), 2.14−1.80 (m, 4H), 1.76 (t, J = 4.4 Hz, 1H), 1.26−1.32 (m, 2H), 1.23 (s, 3H), 1.16 (s, 3H), 1.13 (t, J = 7.2 Hz, 3H), 0.94 (d, J = 7.0 Hz, 3H); ^{13}C NMR ($CDCl_3$, 100 MHz): δ 184.4, 155.5, 136.6, 116.7, 82.9, 73.4, 47.9, 43.1, 37.6, 35.6, 35.1, 26.7, 25.8, 24.8, 21.5, 19.3, 17.3, 10.4; ESI-MS m/z $[M + H]^+$ calcd for $C_{18}H_{29}N_2O_2$ 305.44, found 305.1. HPLC analysis of this material showed exclusively **21**-β.[25]

Hydrolysis of 21-β. *p*-TsOH·H_2O (83 mg; 0.436 mmol) was added to a stirred solution of **21**-β (66 mg, 0.218 mmol) in acetone (2 mL). The mixture was stirred for 15 min and then partitioned between Et_2O and saturated aqueous $NaHCO_3$. The aqueous phase was extracted with Et_2O (twice), and the combined organic extracts were washed with brine, dried ($MgSO_4$), filtered, and evaporated under reduced pressure to give a colorless oil. GC analysis of this material showed a 96:4 mixture of **22**-β/**22**-α.[25] Flash chromatography of the remaining crude material over silica gel using 5:95 Et_2O/pentane gave **22** (25.8 mg, 94%) as a pure, colorless oil. Spectroscopic data was identical to that reported previously.[26]

Acknowledgment. We thank the National Institues of General Medical Sciences, National Institutes of Health (GM-36700 to K.N.H.), National Science Foundation (CHE-0548209 to K.N.H.), Duke University, and Australian Research Council (DP0985623 to E.H.K.) for generous financial support, the NCSA, UCLA ATS, UCLA IDRE, and NCI NF (Australia) for computer resources, and the NCBC for spectroscopic resources. S.E.W. holds an NSF graduate fellowship.

Supporting Information Available: B3LYP geometries and energies, complete citations for refs 17 and 18, experimental procedures, and analytical data for all new compounds. This material is available free of charge via the Internet at http://pubs.acs.org.

(19) Gonzalez, C.; Schlegel, H. B. *J. Chem. Phys.* **1989**, *90*, 2154–2161.
(20) Gonzalez, C.; Schlegel, H. B. *J. Phys. Chem.* **1990**, *94*, 5523–5527.
(21) Scott, A. P.; Radom, L. *J. Phys. Chem.* **1996**, *100*, 16502–16513.
(22) Legault, C. Y. *CYLview, 1.0b*; Université de Sherbrooke: Sherbrooke, Canada, 2009; http://www.cylview.org.
(23) Kallman, N.; Collum, D. B. *J. Am. Chem. Soc.* **1987**, *109*, 7466–7472.
(24) (a) Pratt, L. M.; Khan, I. M. *J. Comput. Chem.* **1995**, *16*, 1067–1080. (b) Pratt, L. M.; Hogen-Esch, T. E.; Khan, I. M. *Tetrahedron* **1995**, *51*, 5955–5970. (c) Pratt, L. M.; Khan, I. M. *J. Mol. Struct.: THEOCHEM* **1996**, *367*, 33–40. (d) Pratt, L. M.; Newman, A.; St. Cyr, J.; Johnson, H.; Miles, B.; Lattier, A.; Austin, E.; Henderson, S.; Hershey, B.; Lin, M.; Balamraju, Y.; Sammonds, L.; Cheramie, J.; Karnes, J.; Hymel, E.; Woodford, B.; Carter, C. *J. Org. Chem.* **2003**, *68*, 6387–6391. (e) Pratt, L. M.; Mu, R. *J. Org. Chem.* **2004**, *69*, 7519–7524. (f) Pratt, L. M. *J. Mol. Struct.: THEOCHEM* **2007**, *811*, 191–196. (g) Pratt, L. M.; Truhlar, D. G.; Cramer, C. J.; Kass, S. R.; Thompson, J. D.; Xidos, J. D. *J. Org. Chem.* **2007**, *72*, 2962–2966. (h) Pratt, L. M.; Nguyen, S. C.; Thanh, B. T. *J. Org. Chem.* **2008**, *73*, 6086–6091. (i) Pratt, L. M.; Jones, D.; Sease, A.; Busch, D.; Faluade, E.; Nguyen, S. C.; Thanh, B. T. *Int. J. Quantum Chem.* **2009**, *109*, 34–42.
(25) See Supporting Information for details.
(26) Hightower, L. E.; Glasgow, L. R.; Stone, K. M.; Albertson, D. A.; Smith, H. A. *J. Org. Chem.* **1970**, *35*, 1881–1886.